AIP | The Journal of Chemical Physics

Radiative and collisional decay of NBr(b 1Σ+,v')

M. A. MacDonald, S. J. David, and R. D. Coombe

Citation: The Journal of Chemical Physics **84**, 5513 (1986); doi: 10.1063/1.449908
View online: http://dx.doi.org/10.1063/1.449908
View Table of Contents: http://scitation.aip.org/content/aip/journal/jcp/84/10?ver=pdfcov
Published by the AIP Publishing

Radiative and collisional decay of NBr($b\ ^1\Sigma^+$, v')

M. A. MacDonald, S. J. David, and R. D. Coombe
Department of Chemistry, University of Denver, Denver, Colorado 80208-0179

(Received 8 November 1985; accepted 11 February 1986)

NBr($b\ ^1\Sigma^+$, v'), $v' \leqslant 10$ is produced by photolysis of BrN_3 at 193 nm. Using this method, radiative decay rates for $v' = 0$, 2, and 5 of the $b\ ^1\Sigma^+$ state were measured and were found to be $\sim 2.5 \times 10^4$ s^{-1}. The rate constant for NBr(b) quenching by collisions with BrN_3 was determined to be 1.57×10^{-10} $cm^3\ s^{-1}$ for $v' = 0$ and slightly faster for $v' > 0$. The nascent vibration distribution of NBr($b\ ^1\Sigma^+$) produced by 193 nm photolysis of BrN_3 was found to be inverted, with a maximum population in $v' = 2$. The overall quantum yield for production of NBr($b\ ^1\Sigma^+$) by the photodissociation is 0.12.

INTRODUCTION

The lowest lying electronic states of the nitrogen halide diatomics are designated as $X(^3\Sigma^-)$, $a(^1\Delta)$, and $b(^1\Sigma^+)$. Angular momentum constraints determine that optical transitions between these states are strongly forbidden. As the mass of the halogen (and thus the nuclear charge) increases, so will the spin-orbit coupling in the molecule, leading to an easing of the constraints and an increase in the radiative decay rate. The radiative rates for NF $a\ ^1\Delta$ and $b\ ^1\Sigma^+$, NCl $a\ ^1\Delta$ and $b\ ^1\Sigma^+$, and NBr $a\ ^1\Delta$ have been reported.[1–4] Coombe and van Benthem[3] discussed the significance of these data. The NBr $b\ ^1\Sigma^+$ decay rate has also been measured from studies of NBr trapped in a low temperature argon matrix.[5] Because of possible perturbations by the matrix, this type of experiment yields only upper limit rate constants. In this paper, we present measurements of rate constants for radiative and collisional relaxation of NBr($b\ ^1\Sigma^+$, v' = 0, 2 and 5) determined from real time gas phase experiments.

Photolysis of ClN_3 at both 193 (ArF) and 248 nm (KrF) produces vibrationally excited NCl(b) and has been used in determinations of the gas phase radiative lifetime of this species.[4] The absorption spectrum of BrN_3 shows three main features centered at 290, 215, and < 195 nm. Attempts to produce NBr(b) by photolysis of BrN_3 at 222 (KrCl) and 308 nm (XeCl) failed, with only $N_2(B \rightarrow A)$ first positive emission being observed.[6] In this paper, we describe the fluorescence generated by exciting BrN_3 in the third band at 193 nm. The NBr ($b \rightarrow X$) fluorescence thus produced was used to determine the NBr (b) radiative decay rate. The nascent NBr (b) vibrational distribution was also determined and was found to be inverted. This result indicates similarities between the production of NCl (b) and NBr (b) from the photolysis of their parent azides, which is discussed in terms of a mechanism involving vertical (Franck–Condon) excitation of these molecules.

EXPERIMENTAL

BrN_3 was generated as described previously,[6] except that the rotameter flow meters used earlier were replaced by mass flow meters (Tylan). The apparatus for the photolysis experiments was also very similar to that described in Ref. 6. The laser was operated on the ArF(193 nm) line. The output of the laser was split with a 2.5 cm diameter spectrosil flat, such that 90% of the beam was directed into the photolysis cell. Fluorescence produced in the cell was detected at 90° to the beam path and was spectrally resolved by a 0.25 m Jarrel–Ash scanning monochromator and a cooled GaAs photomultiplier tube (RCA C31034). The output of the PMT was amplified by a Hewlett–Packard 465 fast amplifier (2 MHz bandwidth) before further analysis. To collect temporaly resolved data, the monochromator was fixed at the wavelength of the feature of interest and the time varying

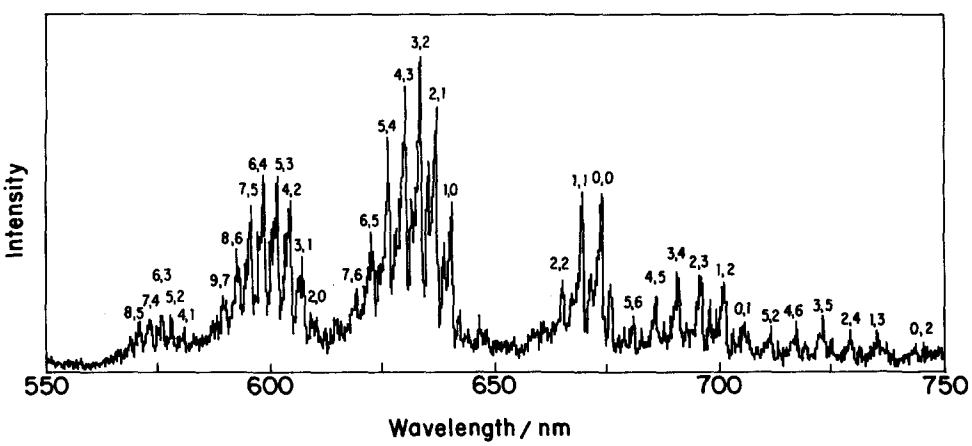

FIG. 1. Spectrum of visible emission produced by the photolysis of BrN_3 at 193 nm. These data reflect emission detected within the first 900 ns after the laser pulse. Bands of the $b\ ^1\Sigma^+ \rightarrow X\ ^3\Sigma^-$ transition in NBr are labeled.

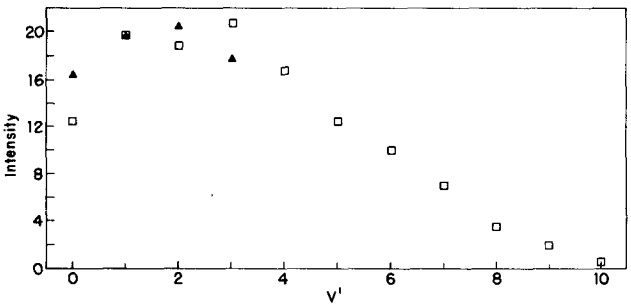

FIG. 2. The vibrational distribution in NBr($b\ ^1\Sigma^+$) produced by 193 nm photolysis of BrN_3. Open squares, distribution determined from integrated intensities within the first 600 ns after the laser pulse. Closed triangles, distribution obtained using relative Franck–Condon factors (Ref. 8).

output of the PMT (after amplification) was digitized, stored, and averaged over successive laser pulses using a Nicolet 1270 signal processing system. The data were then transfered to VAX mainframe computer and analyzed with the aid of an RS/1 statistical package. Spectra of the emissions were recorded by scanning the monochromator as the laser was pulsed at 2 Hz. The signal strength in a selected time interval after the laser pulse was integrated using a dual-channel SR250 gated integrator and boxcar averager (Stanford Research Systems). The data were then analyzed and plotted using an IBM-PC microcomputer operating with the SR265 program supplied with the gated integrator.

The 10% portion of the laser beam deflected by the beam splitter was sent to a reference cell. This cell contained pure I_2 held at 293 K. A 1P28 PMT was attached to the cell to collect the I_2 fluorescence at 90° to the beam. 193 nm light excites I_2 to the D(0_g^+) state which fluoresces with a lifetime of approximately 15 ns [7]; the fluorescence intensity varies linearly with the incident light intensity. These two properties allowed the use of the I_2 cell as both a trigger for the data processing system and as a reference cell to monitor the laser energy. The signal from the 1P28 PMT was fed to the second channel of the gated integrator, where it acted as the trigger. The spectra presented are a ratio of the two channels.

RESULTS

BRN_3 photodissociation

Figure 1 shows the spectrum of fluorescence produced by 193 nm photolysis of BrN_3, within the first 900 ns after

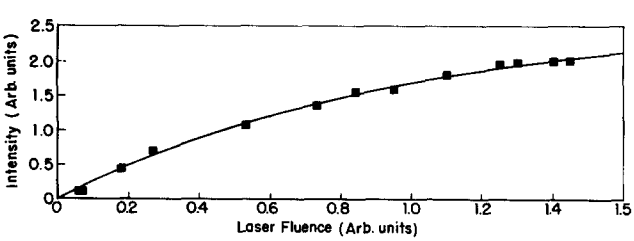

FIG. 3. A plot of the intensity of the 5,4 band of the NBr $b \rightarrow X$ emission vs the incident laser fluence. The intensities were integrated over the 22.4 μs immediately following the laser pulse.

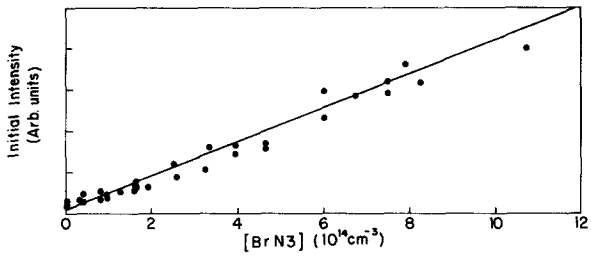

FIG. 4. A plot of the initial intensity (from extrapolation of the decay to $t = 0$) of the NBr $b \rightarrow X$ emission vs the density of BrN_3 for a laser fluence of approximately 100 mJ cm^{-2}.

the laser pulse. This spectrum, which was recorded with a resolution of 0.3 nm, consists largely of NBr $b\ ^1\Sigma^1 \rightarrow X\ ^3\Sigma^-$ transitions. The individual bands were assigned as shown in the figure by using the data presented by Pritt *et al.*[8] Population of vibrational levels of the $b\ ^1\Sigma^+$ state as high as $v' = 10$ is evident. The intensity of light emitted from each v' level within this time interval (900 ns) was integrated over the full range of the recorded spectrum, and the results are shown in Fig. 2 as intensity vs vibrational level. These data indicate a clearly inverted vibrational distribution with a maximum in the $v' = 1$ to $v' = 3$ range.

A number of experiments were carried out to determine the behavior of the NBr $b \rightarrow X$ emission intensity as a function of the incident laser fluence. The data obtained, shown in Fig. 3, indicate that the relationship between these parameters is nonlinear over the full range of fluences employed (0–140 mJ cm^{-2}). The shape of the curve is suggestive of saturation of the BrN_3 absorption, which would have a functional form $I = I_0[1 - \exp(-\sigma E/h\nu)]$, where σ is the absorption cross section and E is the fluence. A fit of the data to this function (shown as a line in the figure) suggests a cross section $\sigma = 1.0 \times 10^{-17}$ cm^2, however, more than four times greater than that noted in previous experiments.[6] Hence, we believe that the curvature in Fig. 3 arises from processes other than saturation, e.g., quenching of the excited NBr by other photoproducts. Certainly there is no evidence of a nonlinear increase in intensity with fluence, as would be the case if the excited NBr were produced by a muliphoton photodissociation process. Figure 4 shows a plot of the initial NBr $b \rightarrow X$ intensity vs the BrN_3 concentration, for low BrN_3 flows and fixed fluence near 100 mJ cm^{-2}. The linearity of the plot indicates that the excited NBr is not produced by collisions between dissociation fragments or between fragments and the parent azide. Taken together, the data in Figs. 3 and 4 offer evidence that excited NBr is an initial fragment of single-photon dissociation of BrN_3.

The time evolution of the emission spectrum in the visible region is shown in Fig. 5. These data were obtained by gating the spectrometer at successively longer delay times after the laser pulse. Two trends are evident in the figure. First, the vibrational distribution in NBr($b\ ^1\Sigma^+$) tends rapidly toward lower v' levels, indicating either fast vibrational relaxation in this state or selective reaction of the higher v' levels. Considerable loss of intensity from the higher vibrational levels is evident for delay times as short as 20 μs. A second trend evident is the growth in intensity of N_2 $B\ ^3\Pi_g \rightarrow A\ ^3\Sigma_u^+$ (first positive) emission, which becomes

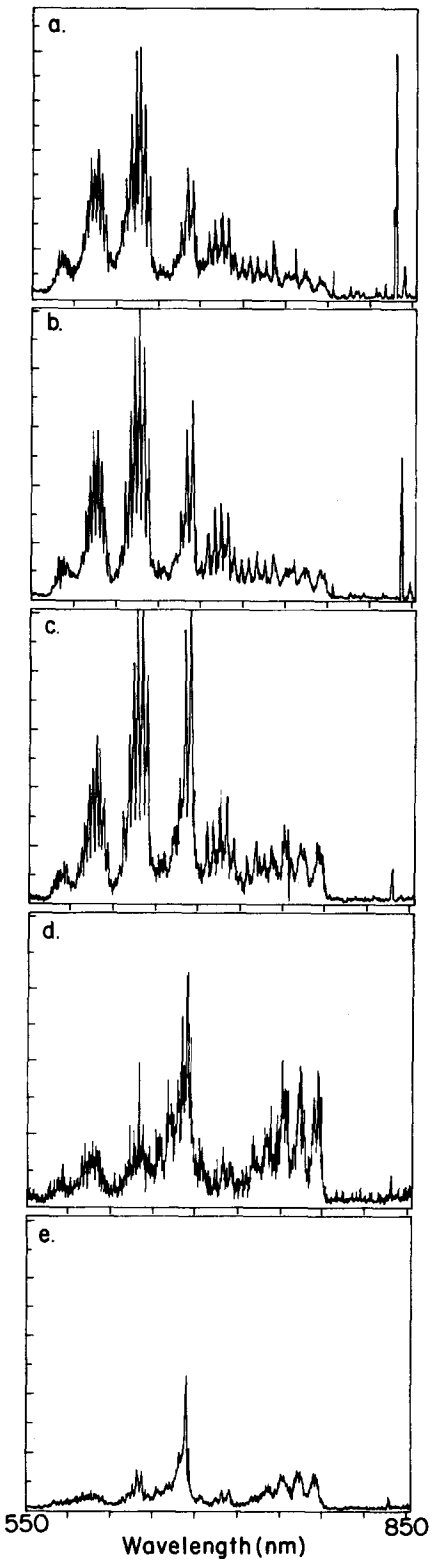

FIG. 5. Time evolution of the visible emission from 193 nm photolysis of BrN_3. (a) 0.0–0.6 μs after the laser pulse, (b) 1.0–1.6 μs after the laser pulse, (c) 3.0–3.6 μs after the laser pulse, (d) 7.5–8.1 μs after the laser pulse, (e) 20.0–22.0 μs after the laser pulse.

dominant after 20 μs. Emission from vibrational levels as high as $v' = 7$ in the $N_2(B\ ^3\Pi_g)$ state was observed, although bands from the lower v' levels appear to be most intense.

The quantum yield of NBr $b \rightarrow X$ emission was measured

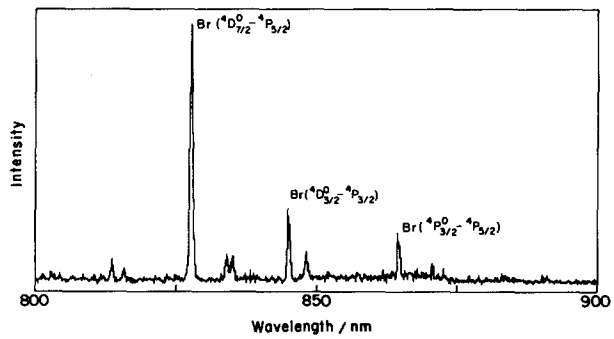

FIG. 6. Spectrum of emission in the 800–900 nm region produced by 193 nm photolysis of BrN_3. Transitions among excited states of bromine atoms are indicated.

by using the photolysis of NH_3 vapor at 193 nm as an actinometer. This technique has been used previously in our laboratory[9] for determination of the $N_2(A\ ^3\Sigma_u^+)$ quantum yield from photodissociation of ClN_3. It relies on a determination of the absolute yield of $NH_2\ ^2A_1 \rightarrow {}^2B_1$ photons from photodissociation of NH_3 reported by Donnelly and coworkers.[10,11] In brief, the time-integrated intensities of NH_2 emission from the photolysis of NH_3 and NBr $b \rightarrow X$ emission from the photolysis of BrN_3 were measured using the same detection apparatus and geometry. The relative yields were determined by deconvolution of these data with the concentrations of the parent molecules, the laser energy, absorption coefficients for NH_3 and BrN_3, and rate constants for radiative and collisional relaxation of $NH_2(^2A_1)$ and NBr($b\ ^1\Sigma^+$). The relaxation data for NBr($b\ ^1\Sigma^+$) are described below. Using this information, and an $NH_2(^2A_1)$ quantum yield of 2.5% as reported by Donnelly *et al.*, we obtained an NBr($b\ ^1\Sigma^+$) quantum yield of 12%. The principle source of uncertainty in this result stems from the $NH_2(^2A_1)$ quantum yield, stated by Donnelly *et al.* to be accurate to within a factor of 3.

The spectra shown in Fig. 5 indicate a narrow, intense feature near 830 nm, not attributable to emission from excited NBr or excited N_2. Figure 6 shows a more clearly resolved spectrum of the 800–900 nm region, recorded under conditions identical to those of Fig. 1. The emission spectrum in this region appears to consist of discrete lines attributable to transitions among excited quartet states of bromine atoms. The assignments are shown in Fig. 6. The states responsible for this emission lie at very high energies. For example, the $4p^45p\ (^4D_{7/2})$ state lies at 75 515 cm^{-1} above the ground state. Figure 7 shows a plot of the intensity of the

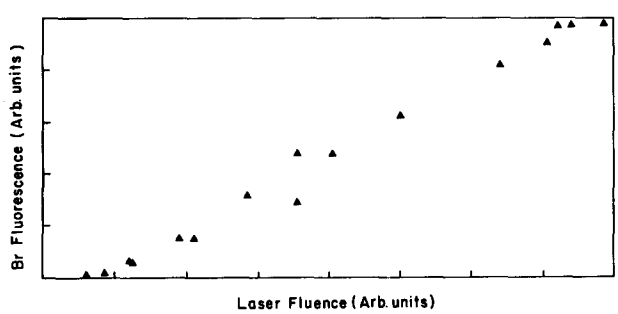

FIG. 7. Intensity of the Br($^4D_{7/2} \rightarrow {}^4P_{5/2}$) emission vs incident laser fluence.

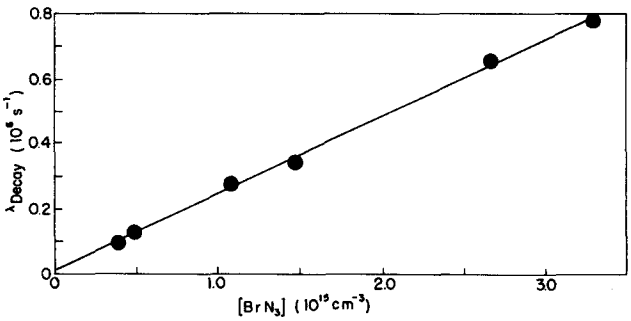

FIG. 8. Time decay of the Br($^4D_{7/2}\rightarrow{}^4P_{5/2}$) emission vs the density of BrN_3. The slope of the line, a linear least-squares fit to the data, yields an apparent rate constant $k = 2.37 \pm 0.05\times10^{-10}$ cm^3 s^{-1}.

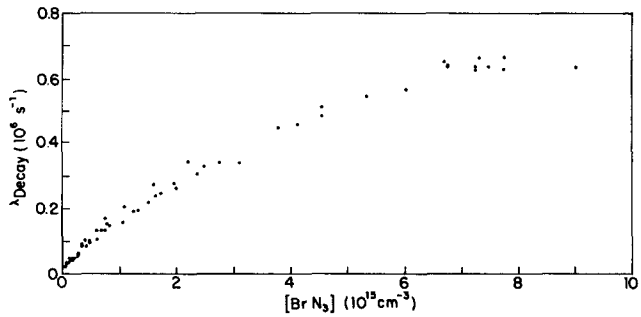

FIG. 10. Decay rate of the fast component of the NBr $b\rightarrow X$ emission (0,0 band) vs the density of BrN_3.

$^4D_{7/2}\rightarrow{}^4P_{5/2}$ feature as a function of the incident laser fluence. The linearity of the plot indicates that the excited bromine atoms are produced by a one-photon event. The time profile of the $^4D_{7/2}\rightarrow{}^4P_{5/2}$ emission was recorded using the apparatus described above. The emission exhibited a rapid rise limited by the finite time constant of the detection electronics, followed by a decay over a few microseconds. Since this is an allowed transition which is presumed to have a large radiative rate, the decay indicates that the excited atoms are formed in a collision process. In order to investigate this process, the decay rate was measured for various BrN_3 densities. The data shown in Fig. 8 indicate a linear relationship between the decay rate and the density of the azide. From the slope of the line, an apparent rate constant $k = 2.37 \pm 0.05\times10^{-10}$ cm^3 s^{-1} is obtained.

Kinetics of NBr($b\ ^1\Sigma^+, v'$) relaxation

The data presented above indicate that NBr($b\ ^1\Sigma^+$) is produced with up to ten quanta of vibrational excitation by the photodissociation of BrN_3 at 193 nm. Rate constants for radiative and collisional decay of excited NBr were measured for the $v' = 0$, 2, and 5 levels. In each case, the time profile of the $b\rightarrow X$ emission exhibited a rise limited by the detection electronics ($\tau\approx0.3\,\mu$s) followed by a double exponential decay, as shown in Fig. 9. Decay rates were determined by fitting the data to a sum of two exponential terms as follows:

$$I(t) = I_0 e^{-t/\tau} + I_0' e^{-t/\tau'}. \qquad (1)$$

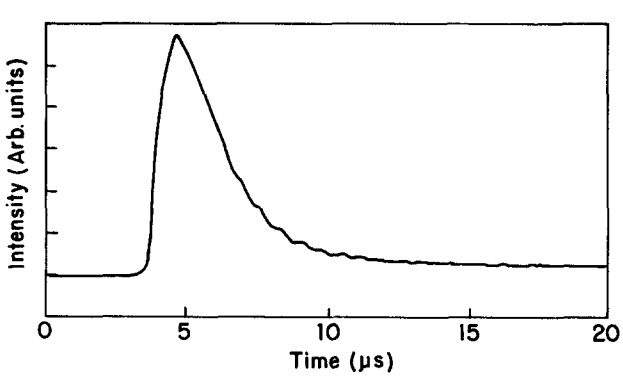

FIG. 9. Time profile of the 0,0 band of the NBr $b\rightarrow X$ emission produced by 193 nm photolysis of BrN_3. [BrN_3] $= 6.7\times10^{15}$ cm^{-3}, [N_2] $= 1.3\times10^{17}$ cm^{-3}.

For the largest BrN_3 densities and bands originating at $v' = 0$, the calculated initial intensity of the slowly decaying component (I_0') was approximately 10% of the initial intensity of the rapidly decaying component (I_0). At lower BrN_3 densities, the relative intensity of the slowly decaying component was much smaller.

In general, each time profile recorded was the average of emission produced by 16 laser pulses. For BrN_3 densities below 1×10^{14} cm^{-3}, however, averaging of as many as 64 individual emission profiles was necessary in order to produce an acceptable signal-to-noise ratio. Figure 10 shows a plot of the measured decay rate of the fast component of the emission from NBr($b\ ^1\Sigma^+, v' = 0$) vs the BrN_3 density, at a constant total pressure of 3.8 Torr. The plot exhibits considerable negative curvature in the region of larger BrN_3 densities. This behavior may well reflect the existence of a finite rise time associated with the slow component of the decay. Since Eq. (1) does not fit such a rise, it would tend to underestimate the true decay rate of the fast component, and as noted above, this effect would be significant only for the larger BrN_3, densities. Another factor which may affect the measured decays for the largest BrN_3 densities is the finite time constant of the electronics. It is unlikely that this time constant could significantly contribute to the curvature evident in Fig. 10 for lower densities, however. Figure 11 shows a plot of the decay rate vs azide density for BrN_3 densities less than 1.1×10^{15} cm^{-3}. The plot is clearly linear in this region. The intercept of the least squares fit to the data in Fig. 10 represents $k_r + k_{N_2}[N_2]$, where k_r is the radiative rate and k_{N_2} is the rate constant for collisional quenching by N_2. The slope represents the rate constant for quenching by

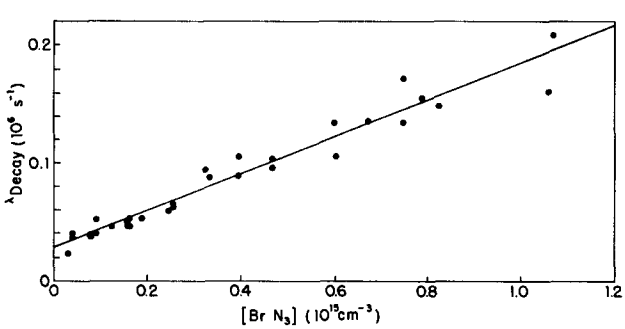

FIG. 11. Decay rate of the fast component of the NBr $b\ ^1\Sigma^+(v' = 0)$ emission vs the density of BrN_3, for low BrN_3 densities.

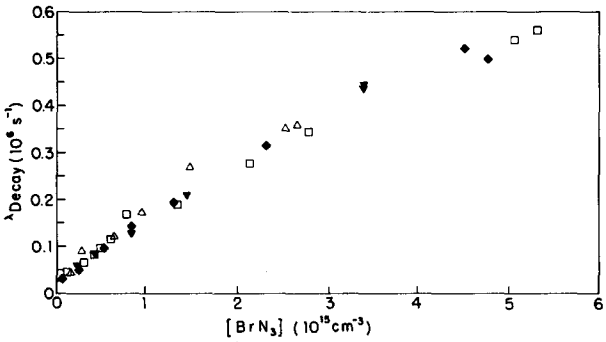

FIG. 12. Decay rate of the fast component of the NBr $b \rightarrow X$ (0,0) emission vs the density of BrN_3, for various N_2 pressures. (□), $[N_2] = 1.28\times10^{17}$ cm^{-3}; (◆), $[N_2] = 1.74\times10^{17}$ cm^{-3}; (▼), $[N_2] = 2.09\times10^{17}$ cm^{-3}; (△), $[N_2] = 2.43\times10^{17}$ cm^{-3}.

BrN_3. From the data, k_{BrN_3} $(v' = 0) = 1.57 \pm 0.06\times10^{-10}$ cm^3 s^{-1}, and $k_r + k_{N_2}[N_2] = 2.8 \pm 0.2\times10^4$ s^{-1}. In order to determine k_r explicitly, it was necessary to measure k_{N_2}. For this purpose, the experiment was modified such that additional N_2 (from the same cylinder as that used to supply the BrN_3 generator) could be added to the photolysis cell. In this way the total pressure could be altered from 3.8 to 7.6 Torr with little effect on the generator. NBr($b\ ^1\Sigma^+$, $v' = 0$) decay rates were measured for a number of various pressures of added N_2. Within the uncertainty of the data, it was found that the intercept of plots of the decay rate vs the BrN_3 density was unaffected by the pressure of added N_2 (see Fig. 12). From these data and those shown in Fig. 11, it was determined that $k_{N_2} < 10^{-14}$ cm^3 s^{-1} and k_r $(v' = 0) = 2.8 \pm 0.5\times10^4$ s^{-1}, corresponding to a radiative lifetime of 36 ± 6 μs.

Similar studies were carried out for emissions on the 5,4 and 2,1 bands of the NBr $b \rightarrow X$ system. The time profiles of these bands also exhibited a double exponential decay, but the relative intensity of the slowly decaying component was much smaller than was found for $v' = 0$, with a calculated initial intensity less than 1% of that of the rapidly decaying component. Radiative rates k_r for $v' = 5$ and $v' = 2$ were found to be quite similar to that for $v' = 0$, as shown in Table I. In view of this similarity, k_{N_2} was not remeasured in these experiments, since vibrational relaxation in collisions with N_2 would serve only to increase the apparent radiative rate (contrary to the results shown in the table). Further, the $v' = 0$ time profiles showed no evidence of pumping by vibrational relaxation. The values of k_{BrN_3} found for $v' = 2$ and $v' = 5$ were slightly larger than that measured for $v' = 0$, suggesting a small enhancement of the rate of this quenching process by vibrational excitation in NBr($b\ ^1\Sigma^+$).

TABLE I. Rate constants for collisional and radiative relaxation of NBr ($b\ ^1\Sigma^+$, $v' = 0, 2, 5$).

v'	k_{BrN_3} (10^{-10} cm^3 s^{-1})	k_r (10^4 s^{-1})
0	1.57 ± 0.06	2.8 ± 0.5
2	2.1 ± 0.1	2.6 ± 0.8
5	3.0 ± 0.1	2.2 ± 0.5

DISCUSSION

The radiative rate of the $b\ ^1\Sigma^+(v' = 0) \rightarrow X\ ^3\Sigma^-$ transition in NBr determined in this work agrees very well with the rate reported by Miller and Andrews[5] from laser-induced fluorescence of NBr trapped in a low temperature matrix. Apparently, the argon matrix used in those experiments had a negligible effect on the electronic structure of the trapped NBr. Our experiments indicate very little change in the radiative rate with increasing v', however, contrary to results from the matrix work. Miller and Andrews observed a lifetime of 25 μs for $v' = 1$ (relative to 40 μs for $v' = 0$), from which these authors inferred the operation of radiationless vibrational relaxation via interaction with the matrix. The present data would appear to confirm this interpretation. This measurement completes a data set comprised of the radiative decay rates of the $b\ ^1\Sigma^+ \rightarrow X\ ^3\Sigma^-$ and $a\ ^1\Delta \rightarrow X\ ^3\Sigma^-$ transitions in NF, NCl, and NBr. This data set is presented in Table II. The effect of increased spin-orbit coupling in the series NF, NCl, NBr on the rates of these forbidden transitions is quite evident. In Ref. 3, this effect was interpreted in terms of the magnitude of spin-orbit matrix elements mixing the $X\ ^3\Sigma^-$, $a\ ^1\Delta$, and $b\ ^1\Sigma^+$ states with one another and with states of the excited configurations $\pi^3\pi^{*3}$ and $\pi^4\pi^*\sigma^*$. Recently, more detailed theoretical treatments of the molecules NF and NCl have been performed in other laboratories.[12,13] All of these efforts seem to indicate that the dominant mechanism in the $b \rightarrow X$ radiative transition involves mixing of the $b\ ^1\Sigma_0^+$ state of the $\pi^4\pi^{*2}$ configuration with the ground $X\ ^3\Sigma_0^-$ state of this same configuration, resulting in the strongly parallel nature of these transitions in NF and NCl.[12,14] The $b \rightarrow X$ transition in NBr is also strongly parallel, suggesting the operation of the same mechanism. In this case, the transition dipole moment should be given approximately by a spin-orbit mixing coefficient multiplied by the difference between the permanent dipole moments of the b and X states. Using a calculation like that described in Ref. 3 (i.e., taking into account one electron interactions only and assuming the states of NBr to be completely covalent), a spin-orbit matrix element of approximately 1267 cm^{-1} is determined for this interaction. Regretably, a radiative rate cannot be calculated from this result since the dipole moments of the $X\ ^3\Sigma^-$ and $b\ ^1\Sigma^+$ states of NBr have not been measured or calculated. If dipole moments of these states in NCl (calculated by Wayne and Colburn)[15] are used in this calculation, an NBr $b \rightarrow X$ radiative rate about 40 times greater than the experimentally measured value is deter-

TABLE II. Radiative rates for the $a\ ^1\Delta \rightarrow X\ ^3\Sigma^-$ and $b\ ^1\Sigma^+ \rightarrow X\ ^3\Sigma^-$ transitions in nitrogen halides.

NX	$k_r(a\ ^1\Delta \rightarrow X\ ^3\Sigma^-)$, s^{-1}	$k_r(b\ ^1\Sigma^+ \rightarrow X\ ^3\Sigma^-)$, s^{-1}
NF	0.2[a]	44.5 ± 3.4[c]
NCl	$4.87 \pm 0.34\times10^2$[b]	$1.59 \pm 0.16\times10^3$[d]
NBr	$1.24 \pm 0.34\times10^3$[b]	$2.8 \pm 0.5\times10^4$[e]

[a] Reference 1.
[b] Reference 3.
[c] Reference 2.
[d] Reference 4.
[e] This work.

TABLE III. Comparison of rate constants for collisional quenching of NCl($a\ ^1\Delta, b\ ^1\Sigma^+$) and NBr($a\ ^1\Delta, b\ ^1\Sigma^+$) by ClN_3 and BrN_3, respectively.

NX	$k(a\ ^1\Delta)$, $cm^3\ s^{-3}$	$k(b\ ^1\Sigma^+, v'=0)$, $cm^3\ s^{-1}$	$k(b\ ^1\Sigma^+, v'=5)$, $cm^3\ s^{-1}$
NCl	$1.27 \pm 0.13 \times 10^{-13}$ [a]	$1.48 \pm 0.04 \times 10^{-12}$ [b]	$1.3 \pm 0.2 \times 10^{-11}$ [b]
NBr	$1.76 \pm 0.04 \times 10^{-11}$ [a]	$1.57 \pm 0.06 \times 10^{-10}$ [c]	$3.0 \pm 0.1 \times 10^{-10}$ [c]

[a] Reference 3.
[b] Reference 4.
[c] This work.

mined. In view of the quadratic dependence of the radiative decay rate on the magnitude of the matrix element and the dipole moment difference, such a large error is not unexpected. Clearly, more extensive calculations of these parameters for NBr are needed.

The rate constants measured for collisional quenching of NBr($b\ ^1\Sigma^+, v'$) by BrN_3 seem to fit a pattern noted in previous studies[4] of analogous quenching processes in the NCl–ClN_3 system. A comparison of quenching rates in the NBr and NCl systems is shown in Table III. The quenching rate constants are larger for the upper v' levels of the $b\ ^1\Sigma^+$ state, suggesting a vibrational enhancement of the rate as was observed for NCl($b\ ^1\Sigma^+$). As in the NCl case, this quenching process is likely to be reactive in nature. The rate constants for NBr(b) quenching are roughly two orders of magnitude greater than those found for NCl(b) quenching by ClN_3, however, an effect which probably arises from the greater fragility of the BrN_3 molecule.[16,17] For example, the thermodynamic strength of the Br–N bond in BrN_3 is less than zero, whereas the Cl–N bond in ClN_3 has a strength of ~ 30 kcal mol^{-1}. In previous measurements of the rates of quenching of the $a\ ^1\Delta$ states of NBr and NCl by the respective halogen azides, the NBr($^1\Delta$) quenching rate constant was also found to be about 100 times larger than that for NCl($a\ ^1\Delta$) quenching. In a similar vein, the relative magnitudes of rate constants for quenching of the $a\ ^1\Delta$ and $b\ ^1\Sigma^+$ states are about the same for NBr and NCl; in each case, the $b\ ^1\Sigma^+$ state is quenched about ten times faster than the $a\ ^1\Delta$ state.

Figure 2 shows that the initial vibrational distribution in the NBr($b\ ^1\Sigma^+$) photofragments is inverted, with a maximum population near $v' = 2$. In principle, a more accurate distribution could be determined from measured intensities of specific bands (Fig. 1) and Franck–Condon factors for the individual transitions. Franck–Condon factors for transitions involving the lower vibrational levels of the $b\ ^1\Sigma^+$ and $X\ ^3\Sigma^-$ states of NBr have been calculated by Itagi,[18] but these values appear to be at odds with experimental observations of NBr $b \rightarrow X$ chemiluminescence. Pritt *et al.*[8] have discussed this discrepancy and presented values of "relative" Franck–Condon factors extracted from experimental data. The triangles in Fig. 2 represent relative vibrational populations in NBr($b\ ^1\Sigma^+$) produced by photodissociation of BrN_3, calculated using these Franck–Condon factors. Clearly, the agreement is good with results obtained from total intensity measurements as described above. In all likelihood, the vibrational excitation of NBr($b\ ^1\Sigma^+$) arises from a mechanism similar to that responsible for the production of vibrationally excited NCl($b\ ^1\Sigma^+$) in the photodissociation of ClN_3.[16] In the latter case, the vibrational excitation observed correlated well with the difference between the known length of the extended N–Cl bond in ClN_3 and the length of this bond in free NCl(b). Although the N–Br bond length in BrN_3 is unknown, its weakness suggests that it is even more extended than the analogous bond in ClN_3. Hence, vibrationally excited NBr($b\ ^1\Sigma^+$) is produced following vertical (Franck–Condon) excitation of BrN_3 in the absorption of the 193 nm photon.

From the time profile of the Br($^4D_{7/2} \rightarrow {}^4P_{5/2}$) emission observed subsequent to the photolysis, it is evident that the excited bromine atoms are produced by a collision process rather than as a direct photofragment. Further, the $^4D_{7/2}$ state, which lies 75 515 cm^{-1} above the ground state of bromine atoms, is not energetically accessible by a direct, one photon fragmentation. The linear dependence of the emission intensity on incident laser fluence rules out multiphoton processes. The data suggest that a mechanism such as the following may be operative:

$$BrN_3 \xrightarrow[193\ nm]{h\nu} NBr(X\ ^3\Sigma^-) + N_2^*, \quad (1)$$

$$N_2^* + BrN_3 \rightarrow Br^*(^4D_{7/2}) + N_2 + N_3, \quad (2)$$

where N_2^* is an unidentified metastable excited state of N_2. Process (1) is feasible given the reported heat of formation of BrN_3[17] and the energy of the 193 nm photon, which are such that an energy of 72 543 cm^{-1} is available to N_2^*. Nitrogen has a number of excited states lying in this energy regime.[19] Since dissociation of BrN_3 at the N–Br bond[6,17] liberates another 3148 cm^{-1}, a total of 75 691 cm^{-1} may be available to the bromine atoms produced by reaction (2), sufficient for production of the $^4D_{7/2}$ state. Because a mechanism such as reactions (1) and (2) requires very specific channeling of a large amount of energy, it is expected that production of N_2^* and consequently Br*($^4D_{7/2}$) is a very minor channel in this photochemical system.

The slowly decaying component of the NBr $b \rightarrow X$ emission and the growth of N_2 first positive emission subsequent to the laser pulse are evidence of reaction mechanisms occurring after the initial photofragmentation. Recent experiments performed in our laboratory[20] have shown that BrN_3 can decompose via a chain mechanism in which Br atoms, N_3 radicals, and excited N_2 metastables act as chain carriers. The chain produces excited NBr($b\ ^1\Sigma^+$) and $N_2(B\ ^3\Pi_g)$ via the reactions

$$Br + N_3 \rightarrow NBr(b\ ^1\Sigma^+) + N_2(X), \quad (3)$$

$$N + N_3 \rightarrow N_2(B\ ^3\Pi_g) + N_2(X), \quad (4)$$

and is initiated by the interaction of BrN_3 with bromine atoms or electronically excited N_2, both of which are likely photofragments in the present experiments. Further, reaction (3) generates NBr($b\ ^1\Sigma^+$) with a much colder vibrational distribution[8] than that shown in Fig. 1, such that NBr $b \rightarrow X$ emission produced by the chain would be most evident for bands involving lower v' levels of the $b\ ^1\Sigma^+$ state. As noted above, this phenomenon was observed in the present experiments.

ACKNOWLEDGMENTS

This work was supported by the National Science Foundation under Grant No. CHE-820533 and by the U.S. Air Force Office of Scientific Research under Grant No. AFOSR-84-0031.

[1]R. J. Malins and D. W. Setser, J. Phys. Chem. **85**, 1342 (1981).
[2]P. H. Tennyson, A. Fontijn, and M. A. A. Clyne, Chem. Phys. **62**, 171 (1981).
[3]R. D. Coombe and M. H. van Benthem, J. Chem. Phys. **81**, 2984 (1984).
[4]A. T. Pritt, Jr., D. Patel, and R. D. Coombe, J. Chem. Phys. **75**, 5720 (1981).
[5]J. C. Miller and L. Andrews, J. Chem. Phys. **71**, 5276 (1979).
[6]R. D. Coombe, J. Chem. Phys. **79**, 254 (1983).
[7]M. Martin, C. Fotakis, R. J. Donovan, and M. J. Shaw, Nuovo Cimento B **63**, 300 (1981).
[8]A. T. Pritt Jr., D. Patel, and R. D. Coombe, J. Mol. Spectrosc. **87**, 401 (1981).
[9]R. D. Coombe, S. J. David, T. L. Henshaw, and D. J. May, Chem. Phys. Lett. **120**, 433 (1985).
[10]V. M. Donnelly, A. P. Baronovski, and J. R. McDonald, Chem. Phys. **43**, 271 (1979).
[11]V. M. Donnelly, A. P. Baronovski, and J. R. McDonald, Chem. Phys. **43**, 283 (1979).
[12]S. J. Havriliak and D. R. Yarkony, J. Chem. Phys. **83**, 1168 (1985).
[13] S. D. Peyerimhoff (private communication).
[14]J. K. G. Watson, Can. J. Phys. **46**, 1637 (1968).
[15]F. D. Wayne and E. A. Colbourn, Mol. Phys. **34**, 1141 (1977).
[16]R. D. Coombe, D. Patel, A. T. Pritt, Jr., and F. J. Wodarczyk, J. Chem. Phys. **75**, 2177 (1981).
[17]R. D. Coombe and C. H-T. Lam, J. Chem. Phys. **80**, 3106 (1984).
[18]S. Itagi, N. R. Shamkuwar, and V. V. Itagi, Indian J. Phys. **45**, 385 (1971).
[19]A. Lofthus and P. H. Krupenie, J. Phys. Chem. Ref. Data **6**, 113 (1977).
[20]T. L. Henshaw, S. J. David, J. V. Gilbert, M. A. MacDonald, D. H. Stedman, and R. D. Coombe (unpublished results).